scientific reports

OPEN

Probing paper ageing by label-free fluorescence lifetime microscopy

Francesca Di Turo✉, Aldo Moscardini, Pasqualantonio Pingue & Francesco Cardarelli✉

Paper ageing is a complex and irreversible process that critically affects materials ranging from packaging to cultural heritage artefacts. While both invasive and non-invasive analytical techniques exist to assess the deterioration of paper, many approaches still present limitations in terms of sensitivity, spatial resolution, or applicability to historical artefacts. Here, we present a fully optical, non-invasive method to monitor oxidation in paper using label-free Fluorescence Lifetime Imaging Microscopy (FLIM). We show that the intrinsic fluorescence lifetime of paper changes with oxidation and that these shifts correlate strongly with FTIR indicators of ageing. Validation was performed on both modern and historical samples subjected to controlled oxidation. This approach represents the first step toward a new diagnostic methodology for monitoring the degradation of paper-based materials in sensitive contexts such as heritage science.

Paper artefacts have played—and continue to play—a pivotal role in human history, serving as primary media for documentation and communication across centuries[1]. However, like many materials, paper undergoes a natural ageing process, which can compromise its structural and chemical integrity. This degradation, driven primarily by hydrolysis and oxidation, poses significant challenges for the long-term preservation of paper-based materials in fields ranging from sustainable packaging to cultural heritage conservation[2,3].

Cellulose is the main component of the paper: it is a biopolymer made up of repeating units of β-(1,4)-D-glucopyranose, linked through interchain secondary valence hydrogen bonds. This results in a multi-layered supramolecular hierarchical structure, with fibres ranging in diameter from 1 to 10 μm. Microfibrils, in turn, are composed of both highly-ordered (i.e. crystalline) domains and disordered (i.e. amorphous-like) regions[4]. Depending on the quality of the raw materials and on the historical period in which the paper artefact was produced, it may also contain hemicellulose, lignin, and various additives aimed at improving its durability and/or writability[5–8]. While the composition of these artefacts can vary, their long-term preservation is invariably challenged by two main deterioration mechanisms, i.e. hydrolysis and oxidation. These processes are not independent and primarily occur in the amorphous regions of cellulose: they catalyse one another, with the formation of carbonyl groups which in turn weaken the glycosidic bonds and make the paper more susceptible to further hydrolysis[9,10]. Hydrolysis is only slightly dependent on temperature but can occur due to the presence of water in the environment or within the sample itself[11–14]. By contrast, oxidation is primarily dependent on temperature[2,9,10,15]. Understanding the mechanisms of paper deterioration remains a fundamental area of research, as cellulose is a key component in a wide range of materials, including those of significant cultural heritage value, such as artworks and manuscripts.

Numerous analytical techniques have been employed to study the degradation of cellulose—the primary component of paper—including Scanning Electron Microscopy (SEM), Atomic Force Microscopy (AFM), X-ray Diffraction (XRD), Nuclear Magnetic Resonance (NMR), and various thermo-analytical methods. In particular, Scanning Electron Microscopy (SEM) and Energy Dispersive X-ray Spectroscopy (EDS), are commonly employed to investigate the structural and surface features of cellulose. These techniques often involve complex sample preparation steps that may be unsuitable for heritage materials[16–19]. On the other side, while Atomic Force Microscopy (AFM) in tapping mode can in principle probe cellulose in native conditions, it can be significantly affected by tip artefacts, potentially losing critical details about the cellulose structure[18–20]. Among the non-imaging techniques, X-ray Diffraction (XRD) is used to characterise crystalline and semi-crystalline cellulose, its degree of crystallinity, and the size of crystallites. XRD does not directly measure cellulose crystallinity but rather provides the mass fraction of crystalline cellulose within the entire sample[20,21]. Furthermore, the sample crystallinity may also include contributions from other crystalline materials besides cellulose, making it challenging to distinguish between the contributions of cellulose and that of other substances[6,21]. Nuclear Magnetic Resonance (NMR) provides insights into the chemical changes and modifications in both amorphous

and crystalline cellulose. Yet, cellulose needs to be dissolved in acid or enzymatic solutions to break hydrogen bonds, making NMR a destructive approach[22,23]. Similarly, thermo-analytical techniques, such as Differential Scanning Calorimetry (DSC) and Thermogravimetric Analysis (TGA), are also destructive, as they probe the thermal properties of cellulose by exposing the sample to high temperatures[24–28]. Although viscosimetry and chromatography are commonly used for cellulose quantification, their applicability to heritage materials is limited for two main reasons: (*i*) in many cases, it is more relevant to assess the overall state of preservation rather than obtain precise quantification; and (*ii*) these techniques are invasive and destructive, making them unsuitable for valuable or irreplaceable items[10,29–35].

Recently, nonlinear optical microscopies—particularly Two-Photon Excited Fluorescence (TPEF) and Second Harmonic Generation (SHG)—have also been employed to investigate photo-induced ageing and flame-retardant treatments in cellulose-based materials. These advanced imaging techniques are often used in combination with FTIR and Raman spectroscopy, which remain among the most widely adopted, non-destructive methods for monitoring the chemical structure of heritage papers. While FTIR and Raman provide valuable vibrational information, the integration of nonlinear optical modalities enables complementary insights into microstructural and molecular-level changes, particularly within the cellulose microfibrils. TPEF and SHG enable label-free imaging of molecular and microstructural changes in cellulose microfibrils, providing additional understanding of degradation mechanisms[36,37]. Moreover, the combination of FLIM with TPEF and SHG has been explored to detect localised variations in nonlinear signals and τ-phase behaviour in cellulose and lignin-rich fibres[36]. While these approaches provide high-resolution structural and functional data, they often rely on complex instrumentation and multi-modal acquisition setups. In contrast, the present study focuses on a standalone FLIM approach that aims to provide a direct, sensitive, and accessible tool for detecting early oxidation-related changes in cellulose, without physical sampling or labelling, and with the potential for adaptation to in situ monitoring.

Optical techniques like UV–Vis spectroscopy and colourimetry provide complementary information about surface degradation. However, these approaches are often limited in their ability to track subtle molecular changes associated with early-stage oxidation, especially without physical sampling[6,38]. In addition, colourimetry and UV–Vis spectroscopy are extensively employed in the characterisation of paper, particularly for monitoring changes in optical properties associated with ageing and degradation. While these techniques are highly effective for evaluating surface colour changes and general material condition, they offer information that complements molecular vibrational spectroscopy and can be valuable components in a multi-technique diagnostic approach[10,39].

Ferrara and colleagues recently applied Fluorescence Lifetime Imaging Microscopy (FLIM) in combination with a carbonyl-selective fluorescent probe to monitor the oxidation of cellulose, where the oxidation stage was inferred from changes in the probe's fluorescence lifetime[40]. In contrast, the approach presented in this study relies on the intrinsic autofluorescence of cellulose, eliminating the need for external probes. FLIM, an advanced imaging technique that maps fluorescence lifetimes across a sample, provides contrast based on the local molecular environment rather than fluorescence intensity alone. This makes it especially effective in detecting subtle chemical and structural alterations, such as those induced by oxidation and degradation processes in cellulose. Inspired by the work of Ferrara et al.[40] and aiming to overcome the limitations of probe-based approaches, we demonstrate that infrared excitation can elicit intrinsic fluorescence from cellulose, and that the corresponding fluorescence lifetime varies in response to paper controlled ageing. Based on this principle, we apply FLIM in the infrared range as a fully optical, non-destructive method to monitor oxidation in both modern and historical cellulose-based samples subjected to controlled ageing in a climate chamber. The molecular interpretation of the observed lifetime shifts is validated through FTIR spectroscopy performed on the same set of samples. This label-free and non-destructive method, enhanced by the use of fit-free and fully graphical phasor-based data analysis, shows great potential to become a powerful and versatile tool for assessing the preservation state of cellulose-based materials, with applications across diverse fields. Unlike traditional analytical techniques, which often require sample preparation or provide only indirect information on degradation, FLIM enables direct, spatially resolved, and sensitive detection of early chemical changes without altering the sample. Importantly, this study represents a first step toward the development of a broader methodology. The observed lifetime shifts associated with ageing not only offer a new layer of information but also suggest promising avenues for future refinement and application. By using the unique capabilities of FLIM in a cultural heritage context, our work introduces an innovative approach that may significantly advance preventive conservation strategies for paper-based materials.

Results and discussion
Label-free FLIM signature of non-oxidised cellulose-based paper
As mentioned in the introductory section, it was recently demonstrated that the oxidation of cellulose can be monitored by measuring the shift in fluorescence lifetime of a probe selective for the carbonyl groups of cellulose[40]. Based on this observation, we wondered whether similar lifetime analyses could be conducted on cellulose-based paper, in the absence of any destructive labelling, i.e. by exploiting intrinsic cellulose fluorescence. To investigate this, we used paper made of pure cotton, free from optical brighteners, but containing an alkaline reserve.

Indeed, it is well known that cellulose autofluorescence can be stimulated in the UV-Vis range, as Kulpinski and co-workers described in their research[41]. More specifically, it was shown that pure regenerated cellulose absorbs light in the 220–400 nm range of wavelengths, then emitting most of the radiation in the 400–600 nm range. Building on this, we chose to test cellulose excitation in the infrared range (700 nm) exploiting 2-photon absorption at approximately twice the excitation wavelengths of those characterized by 1-photon measurements:

this, in principle, not only reduces the excitation energy on the sample and guarantees deeper penetration of light but also addresses the scarce availability of pulsed laser sources in the far-UV range.

To optimize signal detection and prevent overflow in the system, we employed a dichroic mirror with a cut-off at 570 nm, complemented by a filter centred at 510 nm with a ± 40 nm range. The fluorescence emission was then captured using a high-resolution 30x silicon immersion objective (NA = 1.0), which provided an ideal balance of magnification and numerical aperture for these measurements. Each FLIM image was acquired with a 512 × 512-pixel resolution, using a laser power set to 0.4% to minimize photobleaching while maintaining sufficient signal strength. Depending on the fluorescence emission of the sample, between 20 and 30 frames were collected to ensure robust averaging, with the scanning speed set at 10 µm/s for consistent data quality across all measurements.

The structure of cellulose fibres, captured using a 30x objective lens at the lowest digital zoom, is shown in Fig. 1a, alongside its fluorescence decay representation as a phasor plot. In this measurement, the lifetime signal is composed of three main contributions: the background signal (highlighted in blue), characterized by longer lifetimes; the fibre signal (purple); and highly fluorescent spots (yellow), which cause a shift toward shorter lifetimes. At this digital zoom, the cellulose signal appears complex and includes components that may not be diagnostic of the cellulose fibres themselves.

To isolate the cellulose fibre signal and minimize the influence of background signal and high fluorescent spots, we conducted the analysis exclusively at higher digital zoom focused on individual fibres, as shown by the fibre analyses of squares 1, 2, and 3 in Fig. 1a. Acquiring the lifetime signal at these digital zooms enables a cleaner signal that depends solely on the fibre's contribution, as evidenced by the corresponding phasor plots for the three analysed fibres.

Furthermore, it is evident that the fluorescence lifetime signal remains consistent between the low-magnification image (Fig. 1a, b) and the high-magnification views of selected fibres (Fig. 1c, d, e, regions 1–3). At lower magnification, the field of view includes a larger portion of the sample, which increases the likelihood of capturing unwanted signals from non-fibre regions—such as background, surface impurities, or other highly fluorescent contaminants. This introduces additional noise and can distort the lifetime distribution. By contrast, acquiring images at higher magnification with digital zoom enabled us to isolate individual fibres and significantly reduce interference from these undesired components. Thanks to this targeted microscopic visualisation, we were able to identify and exclude bright spots that could otherwise skew the analysis. These regions, which show up clearly in the composite phasor plot (Fig. 1b), were deliberately omitted to ensure
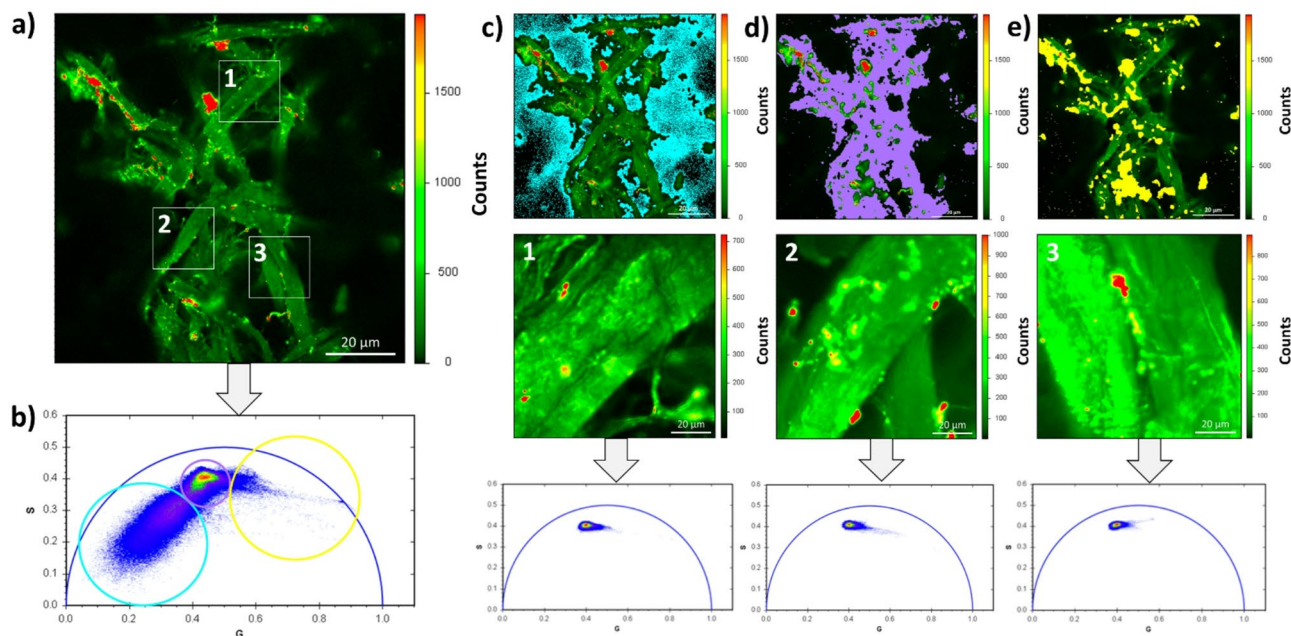

Fig. 1. **(a)** Fluorescence lifetime image of cellulose fibres acquired at low magnification, and **(b)** the corresponding phasor plot representing the overall fluorescence response of the sample. The global signal of the phasor plot shown in (b) includes contributions from: **(c)** the background with longer lifetimes (highlighted in light blue), **(d)** the cellulose fibres (highlighted in purple), and **(e)** highly fluorescent spots associated with shorter lifetimes (highlighted in yellow). To minimise interference from components not directly related to the cellulose matrix, high-resolution FLIM imaging was performed using a 30× objective, combined with 10× digital zoom, to selectively analyse individual fibres. Regions of interest (1, 2, and 3 in panel a) were selected accordingly and are shown at higher magnification in the lower panels of (c–e). The associated phasor plots (bottom row) confirm consistent fluorescence lifetime distributions for the selected fibres. These values are stable across magnification levels and are representative of the intrinsic lifetime of the cellulose fibres of interest.

that the lifetime values reflect only the cellulose fibres of interest, especially at higher digital zoom. The use of phasor plot analysis further enhances this approach by enabling intuitive and robust discrimination between different lifetime populations within the image. Representing fluorescence lifetime decays in the phasor domain offers several advantages, including fit-free analysis, model independence, and simplified interpretation. In this representation, each decay is transformed via a Fourier algorithm into a position in the phasor plot, where mono-exponential decays lie on the universal semicircle (blue arc in Fig. 1b), while multiexponential decays fall within it (see *Materials and Methods*). As expected for cellulose, the signal appears inside the semicircle, reflecting its characteristic multiexponential decay behaviour[42].

The FLIM signature of cellulose-based paper changes with controlled oxidation in a climatic chamber

After establishing the fluorescence fingerprint of non-oxidisd cellulose-based paper, an accelerated oxidation protocol was implemented to track the related modification. The use of high temperatures to induce aging is a well-established method in the literature for studying the deterioration mechanisms of cellulose[25,43,44]. We accelerated the oxidation processes by following the ISO 5630-1:1991 standard, which outlines the method for artificial ageing of paper in a dry-heat environment. According to this procedure, subjecting the sample to dry heating for 3 days at 105 °C is equivalent to approximately 25 years of ageing[44,45]. Moreover, under these conditions, oxidation becomes the predominant deterioration process, as hydrolysis is primarily influenced by the inherent moisture content of the paper[9]. However, we are fully aware that deterioration in real-world scenarios involves a broader range of environmental factors (such as humidity, light exposure, and pollutants);therefore this work represents the first application of a novel FLIM-based methodology to monitor cellulose oxidation. To ensure experimental control and isolate the effect of oxidation, we focused on a single, well-defined ageing factor—temperature-induced oxidation—with the aim of validating the approach before extending it to more complex and realistic conditions.

Phasor-FLIM reveals early oxidative changes in paper undetectable by SEM-EDS, highlighting its value as a complementary diagnostic tool (Fig. S1). This can be appreciated in Fig. 2(a, b), which shows the phasor plot of the control sample alongside samples aged to simulate up to 200 years of deterioration. Measurements were conducted on at least three different fibres to obtain average values and associated errors. Detailed fluorescence lifetimes for both the control and aged samples are provided in Table S1. The distinct separation of lifetime signals observed in Fig. 2a, b underscores the capability of this approach to track cellulose-based paper ageing. Notably, the average fluorescence lifetime decreases from 3.22 ns in the control sample to 2.53 ns in the sample oxidised to simulate 200 years of ageing (Table S1). By contrast, SEM-EDS analysis and EDS data (Fig. S1 and Table S2) show no visible signs of ageing in the paper structure and/or composition.

Validation of FLIM results by FTIR: the role of cellulose ageing

At this point, to probe whether the shifts in the fluorescence lifetime of cellulose fibres observed after incubation in the climatic chamber are effectively correlated with molecular modifications (i.e., oxidation) of cellulose-based paper, we performed FTIR spectroscopy on the samples at different stages of apparent ageing (Fig. 2c, d). FTIR spectroscopy was selected as a validation technique for several reasons. First, it is a non-invasive and widely accepted method in heritage science for assessing the condition of manuscripts and paper-based materials[6,30]. Second, its versatility allows for straightforward post-ageing analysis of the same samples without the need for additional preparation. Most importantly, our interest lies in evaluating the overall ageing behaviour of cellulose-based materials rather than quantifying specific degradation compounds. This aligns with the broader goal of developing a methodology applicable in heritage contexts, where non-destructive tools that capture general trends in material degradation are especially valuable. Notably, we observed a consistent shift in fluorescence lifetime that correlates with FTIR indicators of ageing, reinforcing the validity of our optical approach.

It is important to note that we are analysing processed cellulose rather than pure native cellulose. While our samples consist of pure cotton paper without optical brighteners, spectral interpretation can still be influenced by factors such as the coexistence of crystalline and amorphous cellulose, which is characteristic of paper materials. Examining the spectra in Fig. 2c, several characteristic features can stand out, especially in the diagnostic region between 1800 cm^{-1} and 1600 cm^{-1}, used to monitor oxidation and deterioration in paper and cellulose[29]. The presence of residual water is indicated by a broad band around 3272 cm^{-1}, corresponding to the stretching of O-H bonds in alcohols, along with a prominent peak at 2850 cm^{-1}, representing C-H stretching. These signals are typically observed due to the residual moisture, but their contribution is minimal in our dry ageing conditions.

In the 1300–1400 cm^{-1} range, bending vibrations of C-H bonds adjacent to carboxyl groups (α position) are seen, while the peak at 1030 cm^{-1} is attributed to C-O stretching in alcohols.

As ageing progresses, we observe the increasing intensity of the band 1311 cm^{-1}, associated with the C-H scissoring or C-O stretching. Also the region between 1400 and 1280 cm^{-1} becomes more pronounced with accelerated dry ageing in climate chamber. In particular, the peak around 1420 cm^{-1} increases from the control to the 200 years of ageing. Peaks at 1500 cm^{-1} and 1543 cm^{-1} suggest the presence of carboxylic acids, which are further evident as the sample ages.

Focusing on the diagnostic region between 1800 cm^{-1} and 1600 cm^{-1} (Fig. 2d), we notice several indication of a deterioration which, under our dry ageing conditions, can be primarily attributed to oxidation. The peak at 1644 cm^{-1}, corresponding to the stretching of carbonyl bonds (ketones or aldehydes) intensifies with ageing, indicating the oxidation of alcohols into carbonyls. Over time, the signal shifts, with dikentone conjugation causing the carbonyl stretch to appear around 1680 cm^{-1} instead the usual 1712 cm^{-1}[29] The appearance of new peaks, particularly between 1740 cm^{-1} and 1750 cm^{-1}, correlates with the formation of carboxylic acid as oxidation progresses. The gradual intensification of carbonyl peaks and the emergence of additional bands at
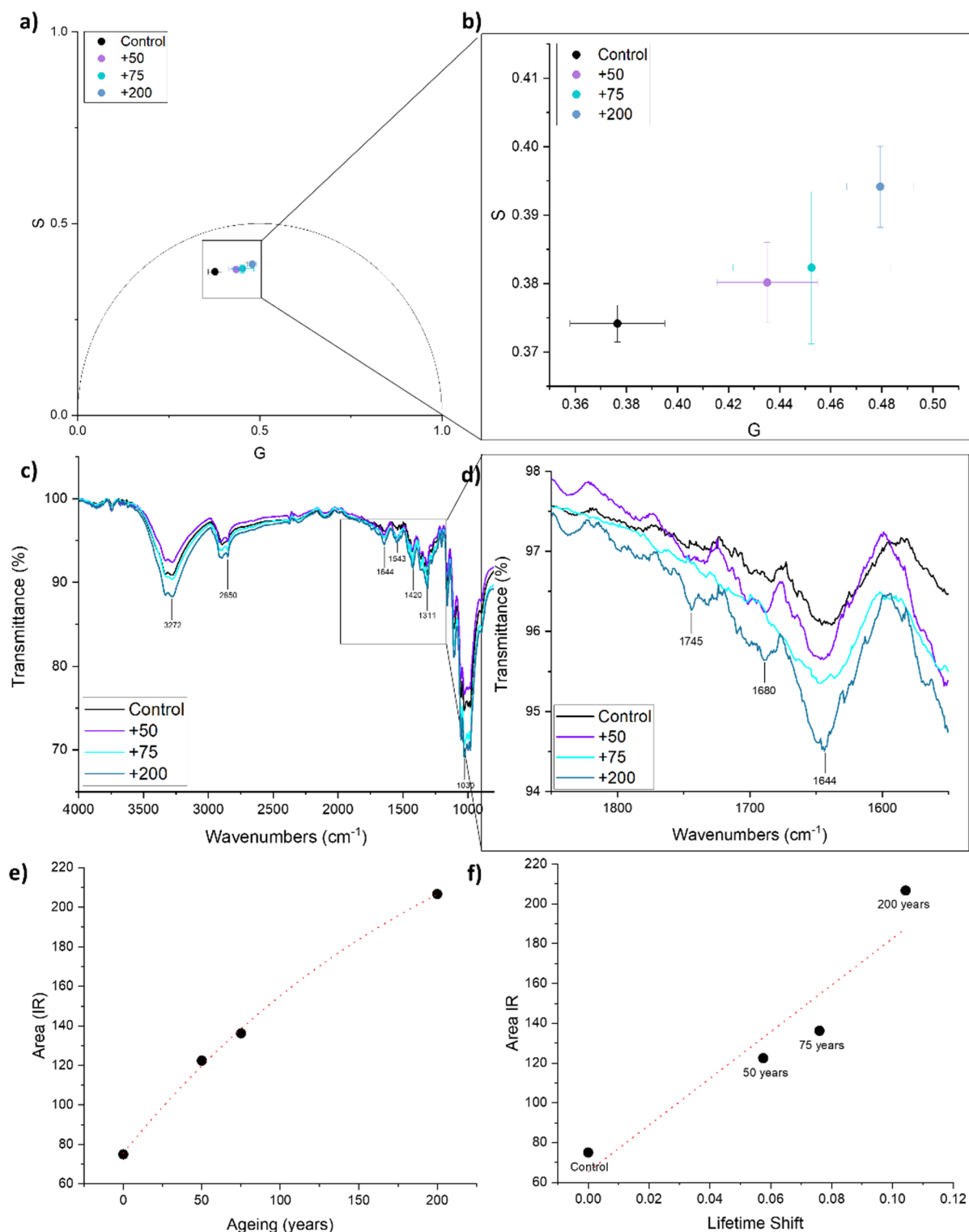
Fig. 2. (**a**, **b**) FLIM analysis of the control sample and of those aged to simulate 200 years, illustrating the progressive shift in fluorescence lifetime as a result of ageing. Measurements were conducted on at least three different fibres to obtain average values and associated errors. (**c**, **d**) FTIR-ATR spectrum of the samples. Data were acquired from 3700 to 650 cm^{-1}, with a zoom highlighting the region of interest where paper deterioration becomes evident. The spectral resolution was 4 cm^{-1}, and 256 scans were acquired for the background. (**e**) The relationship between paper ageing and the calculated IR areas in the spectral region between 1600 and 1800 cm^{-1} (adjusted R-square = 0.99377). The peak areas in the region of interest diagnose the progression of oxidation, confirming that the samples are undergoing alteration, which is also visible through the lifetime shift in the phasor plot. (**f**) The data from FLIM and FTIR show to the correlation between the lifetime shift obtained from FLIM analysis and the calculated peak areas in the 1595–1800 cm^{-1} range. The Pearson's coefficient is $R = 0.94832$.

lower wavenumbers, such as around 1675 cm^{-1} for diketone at C(2) and 1750 cm^{-1} linked to enol formation, reflects the ongoing oxidation of the cellulose-based paper.

In the 200-year aged sample, further bands appear between 1745 cm^{-1} and 1740 cm^{-1}, indicating the formation of carboxyl groups, possibly representing further oxidation of ketones and aldehydes. The overall increase in band intensities, particularly in the 1600–1800 cm^{-1} range, support the progression of oxidation as a primary process in the ageing of the paper sample. The relationship between the increasing band intensity and aging is shown in Fig. 2e.

Then, given the consistency between the FLIM and FTIR results, we next investigated whether a clear correlation exists between the oxidation process, the observed lifetime shift, and the FTIR areas associated with oxidation. The correspondence between the IR integral of oxidation-related groups and fluorescence lifetime is give in Fig. 2f. The graph illustrates the shift in fluorescence lifetime of cellulose as a result of oxidation, alongside the increase in the IR peak area within the diagnostic region. This relationship confirms that the observed lifetime shift can be directly linked to the oxidation process. Furthermore, the correlation between the fluorescence lifetime shift and the IR peak areas obtained through FTIR validates the use of FLIM as a reliable method for monitoring cellulose oxidation. Although pH measurements reflect ageing in a slower and less sensitive manner (Fig. S2), they still support the overall trend of degradation over time, consistent with the lifetime shifts observed by FLIM.

FLIM analysis on historical paper

Given that historical papers differ significantly from modern ones in terms of composition, fabrication techniques, and natural ageing processes, we apply the previously tested method to historical samples to verify its robustness and diagnostic relevance across diverse case studies. Historical paper, in fact, has a complex conservation history, and the raw materials may differ, with contamination arising from manual production processes and usage across the centuries. In this view, we analysed a sample from the Salviati Archive of the Scuola Normale Superiore, dating back to the 19th century. The Salviati Archive offers a wealth of administrative and economic records that span several centuries, providing crucial insights into the management of vast estates and financial activities of the Salviati family, one of the most influential aristocratic families in Tuscany. These documents, dating from the 12th to the 19th centuries, include detailed accounts of land holdings, income registers, contracts, and transactions, reflecting the complex operations involved in estate management during this period. A sample of paper analysed in this study originates from a 19th-century economic register found in the archive, contributing to the broader understanding of historical record-keeping practices and material use in the administration of large estates in early modern Italy. These manuscripts are stored in an archive without climate control, and therefore, no preventive conservation measures are in place. As a result, their deterioration is due to fluctuations in temperature, variable humidity, and other adverse environmental conditions. Investigating the microstructure of historical paper is always valuable, as it can provide insights into both the original papermaking techniques and the current conservation status of the material[1,46]. Microstructural characteristics such as fibre orientation may reveal details about the sheet-forming method and the type of mould used, while porosity can be linked to historical drying or pressing techniques[47]. The presence of inclusions—such as mineral fillers, unprocessed fibres, or residues from sizing agents—can shed light on the composition and quality of the raw materials employed[48,49]. These features not only offer a window into historical manufacturing practices but also influence the paper's vulnerability to environmental stressors and ageing mechanisms[46,50]. As reported in Fig. S3 that shows backscattered electron images of the historical sample before ageing (Fig. S3a) and progressively aged to simulate 75 and 200 years of deterioration (Fig. S3b, c).

Here, we use SEM-EDS to obtain complementary information on the morphological and elemental features of the paper samples. SEM offers high-resolution imaging of the surface, allowing for the assessment of physical changes in fibre structure or morphology induced by ageing protocols. Meanwhile, EDS enables the detection of elemental composition, which can reveal the presence of inorganic additives or contaminants that might influence degradation processes. Although SEM-EDS is not sensitive to organic molecular changes like those detected by FLIM or FTIR, it remains a valuable technique for characterising structural integrity and identifying potentially influential exogenous elements. In this context, SEM-EDS served to confirm that no significant morphological alterations or inorganic contaminants were introduced during the artificial ageing protocols, thereby supporting the interpretation of fluorescence lifetime shifts as being predominantly due to intrinsic chemical changes in cellulose. Studying the microstructure then suggests thet the historical paper has greater porosity compared to modern cellulose paper (Fig. S1), with the fibre network becoming less dense as the ageing process progresses. In all samples, the fibres appear long and randomly distributed, indicating high-quality raw material, likely predominantly cellulose (linen or cotton), in accordance with century-specific paper production practices. In fact, paper originally made from long cellulose chains will have a long structure and be less vulnerable to deterioration[14]. Moreover, the random distribution suggests manual manufacturing, as machines introduced later tended to impart a preferential direction to the fibres. The fibre density begins to diminish during ageing, while the porosity increases. The presence of white dots scattered randomly on the surface, common to all samples, may be attributed to both exogenous material (powder) and paper fillers, such as glue or additives[46,50]. Aside from some breakage in smaller fibres, it is not possible to detect the progressive oxidation of cellulose with SEM-EDS. EDS (Table S3) identified several elements in the microstructure, including Mg, Si, Na, K, and Ca, primarily originating from commonly added paper additives such as kaolin [Al$_2$Si$_2$O$_5$(OH)$_4$], calcium carbonate [CaCO$_3$], magnesium carbonate [MgCO$_3$], and alum [KAl(SO$_4$)$_2$]. Silica may originate from silicon-based compounds that can be naturally present in paper, found abundantly as a component of the plant fibres themselves[17,51–53]. The presence of chlorine, even if in low quantities, can also be considered an impurity associated with surface dirt, even if Cl may oxidize the cellulose and produce carboxylic groups, as detected in the FTIR analysis (*vide infra*). The incorporation of a pH-increasing filler like calcium carbonate and the

utilization of alum alternatives can mitigate the acidity of the final paper. Figure 3a, b and Table S4 illustrate the lifetime shift of the historical sample, demonstrating that cellulose deterioration can be tracked as ageing progresses in this case as well. While pH measurements (Fig. S4) remain relatively stable around 7.6–7.7 within the range of experimental error, indicating minimal acidification, phasor-FLIM analysis reveals detectable changes in fluorescence lifetime associated with early-stage oxidation (Fig. 3a, b). This highlights the higher sensitivity of FLIM in capturing initial molecular alterations that precede measurable shifts.

FTIR analysis of the historical sample showed diagnostic shifts in the 1800–1600 cm^{-1} region consistent with oxidation (Fig. 3c, d). Although the peak positions differed slightly from those in modern paper due to compositional differences, the correlation between FTIR peak area and FLIM lifetime remained strong ($R = 0.96$; Fig. 3e, f). This confirms the method's robustness across different materials. Nevertheless, despite these compositional differences, we focused on the spectral range between 1800 and 1000 cm^{-1}, paying particular attention to the differences observed in aged samples. Although the presence of residual water in the samples may contribute to certain peaks, particularly in the O-H stretching region (around 3272 cm^{-1}), the drying process prior to ageing and controlled dry conditions (105 °C) employed during the accelerating ageing, reduces the water's impact on the signals. As a result, the observed spectral shift in the diagnostic region, particularly the increase of peak intensity associated with oxidation (such as the carbonyl group around 1644 cm^{-1}), are primarily attributed to the oxidation process itself, rather than water interference. A shift in lifetime is noticeable after just 50 years of simulated ageing, consistent with the formation of oxidation-related functional groups in FTIR spectrum (Fig. 3d). Despite the shift in these diagnostic peaks for historical paper, the correlation between the increase in peak areas and the progression of paper deterioration remains valid (Figs. 2e and 3e). Furthermore, although the lifetime shift follows a different trend compared to the contemporary cellulose-based paper sample, a correlation between the FTIR and FLIM data is still observable, further supporting the potential of this method across different case studies (Fig. 3f).

While demonstrated here on two paper samples with different conservation histories, this work highlights the potential versatility of FLIM in analysing paper-based materials with heterogeneous compositions. Overall, the agreement between the two independent techniques supports the possibility to further develop this method. FLIM reveals a degradation pattern that reflects the oxidative changes induced by controlled ageing, thereby enabling, for the first time, observation of the optical signature of autofluorescent cellulose and its progressive shift during ageing.

Conclusions

This research presents a fully optical, label-free, and non-invasive approach for tracking the deterioration of cellulose-based paper due to oxidation processes using FLIM in the infrared range. To assess the broad applicability of the method, we applied it to both contemporary handmade cellulose paper and a 19th-century sample from the historical Salviati Archive at the Scuola Normale Superiore. We optimised the experimental setup to capture intrinsic fluorescence without external labelling and monitored the emission across the full paper matrix. Rather than isolating cellulose fibres, our analysis reflects the entire composition of the paper, including possible additives such as sizing agents, fillers, or starch. This choice was deliberate, as our goal was to assess how real, complex paper systems evolve with ageing—more in line with the practical needs of heritage science.

Subsequently, we demonstrated that the fluorescence lifetime shifts in response to the progression of paper oxidation induced by a dry heat protocol performed in a climatic chamber. The molecular interpretation of ageing—driven primarily by oxidation—is supported by FTIR data, which reveal significant chemical changes in the paper during accelerated oxidation under dry conditions. These findings confirm the observations made through FLIM, reinforcing the idea that the deterioration process is predominantly due to oxidation rather than hydrolysis or moisture-related effects.

Importantly, this work represents the first step towards: (i) defining the autofluorescence behaviour and characteristic lifetime response of cellulose-based paper materials; and (ii) establishing a correlation between fluorescence lifetime shifts and the progression of ageing and degradation. While we recognise that the fluorescence signal may be influenced by components beyond cellulose alone, our methodology focuses on understanding the material's behaviour as a whole. Building on this foundation, the methodology could be further developed to create a reference database or calibration curves that enable the estimation of a sample's degree of ageing. The development of such tools requires the use of controlled ageing protocols to systematically study lifetime shifts under defined conditions, acknowledging that real-world degradation processes may depend on a wide variety of environmental and material-specific factors. Although the current implementation involves sample collection, the method remains fundamentally non-destructive, as it does not alter or consume the material and requires no external labelling. By applying the advantages of FLIM—its label-free, spatially resolved, and sensitive detection capabilities—this study introduces an innovative diagnostic tool for cultural heritage science. With future integration into a portable setup, the approach has the potential to become fully non-invasive and ideally suited for *in situ* applications on heritage objects, significantly advancing preventive conservation strategies.

Materials and methods
Materials

Handmade paper samples (1×1 cm) made from pure cotton cellulose (Paper & People, Srl, Milan, Italy), free of optical brighteners and containing an alkaline reserve for pH buffering, were used to establish the analytical protocol. Additional 1×1 cm historical paper samples were obtained from a 19th-century manuscript housed in the Salviati Archive at the Scuola Normale Superiore (Pisa, Italy). These samples were excised from the edges of
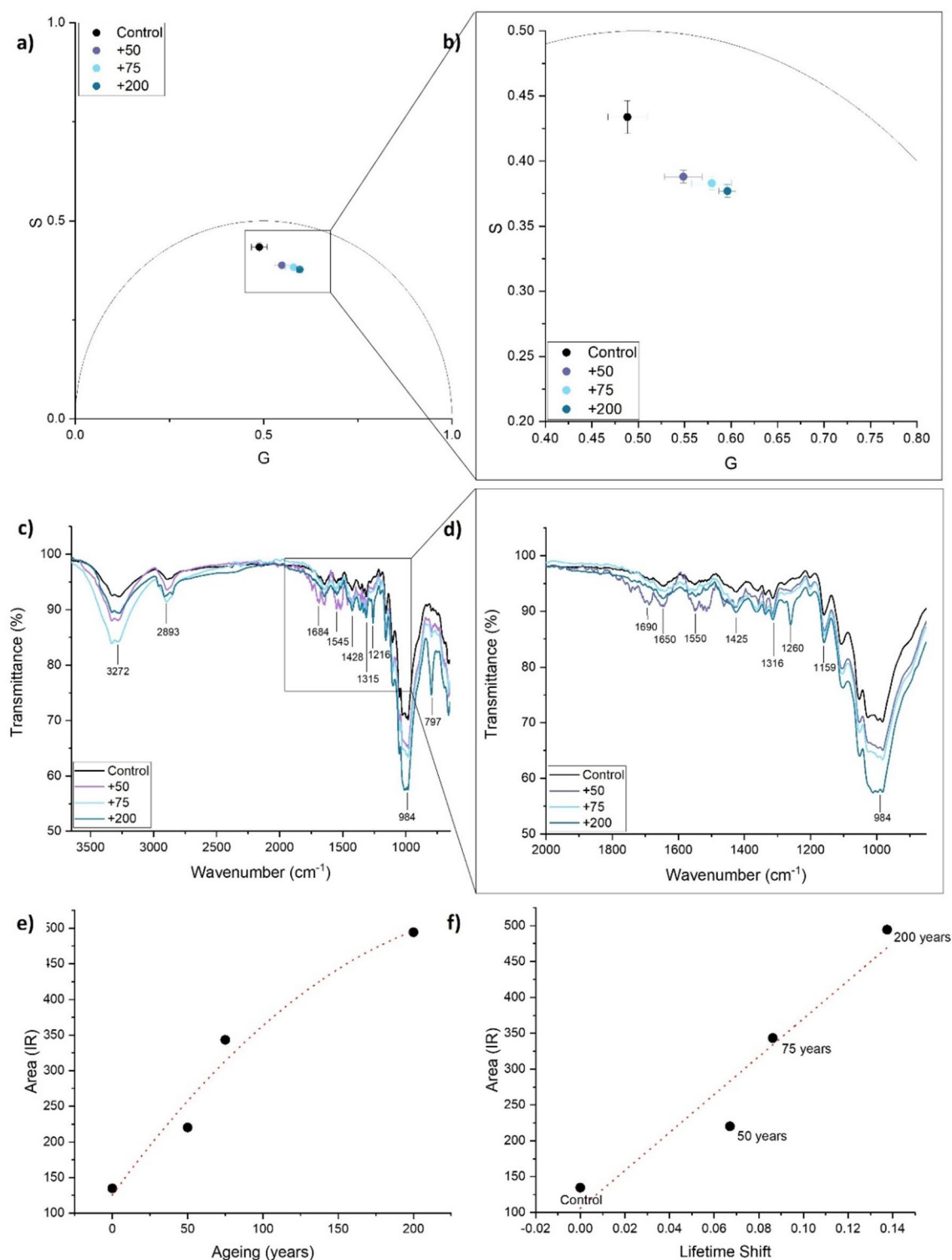
Fig. 3. (**a**, **b**) FLIM analysis of the historical paper (1800s) from the historical archive of Salviati (Scuola Normale Superiore). The control sample is progressively oxidised up to the simulation of 200 years of ageing, highlights the progressive shift in fluorescence lifetime as a result of deterioration. Measurements were conducted on at least three different fibres to obtain average values and associated errors. (**c**, **d**) FTIR-ATR spectrum of the samples. Data were acquired over the range 3700 to 650 cm^{-1}, with a focus on the region of interest (spectral range between 1800 and 1000 cm^{-1}) where paper deterioration becomes evident. The spectral resolution was 4 cm^{-1}, and 256 scans were acquired for the background. (**e**) The relationship between paper deterioration and the calculated IR peak areas in the spectral region between 1600 and 1800 cm^{-1} (Adj. R-square = 0.90361) demonstrates that, in this case as well, the increase in peak area corresponds to the progression of aging, following the ISO 5630-1:1991 procedure to promote the oxidation process. (**f**) FLIM and FTIR data are correlated, resulting in a linear fit with Pearson's correlation coefficient $R = 0.96174$.

the sheets, avoiding written areas. All specimens were in stable condition and did not require special handling precautions.

Sample preparation and accelerated paper ageing

Before any analysis, the control sample was dried at 105 °C for 24 h to minimise the presence of residual moisture. Accelerated ageing was then performed in a climate chamber (Espec TCC-150 W, DJK Europe GmbH, Germany) under dry heat conditions (105 °C) according to ISO 5630-1:1991, which equates 3 days of thermal exposure to approximately 25 years of natural ageing[44,45,54]. Samples were aged for 3, 6, 9, 12, and 24 days, corresponding to 25, 50, 75, 100, and 200 years of simulated ageing, respectively. The same protocol was applied to both modern and historical paper samples. Recognising that accelerated ageing protocols do not fully replicate the complexity of real-world ageing, they are nevertheless essential for systematically assessing lifetime shifts under controlled conditions. To assess and minimise water interference in FTIR spectra, we compared samples under three drying conditions: (i) untreated (as received), (ii) oven-dried at 105 °C for 4 h, and (iii) vacuum-dried (10 mbar) at 105 °C for 4 h. FTIR spectra confirmed a substantial reduction in O–H and H–O–H bands after both drying procedures, indicating minimal residual water in the analysed samples (see Fig. S5). These bands are significantly reduced in both dried samples, which also show highly similar spectra. This confirms that residual water content is minimal in the dried samples, and the FTIR signals reflect structural features of cellulose rather than water-related artefacts. Although the FTIR and FLIM measurements were performed under ambient environmental conditions, they were carried out immediately after the ageing protocols and drying steps, minimising the material's exposure to ambient humidity and ensuring the reliability of the spectral data.

Fluorescence lifetime imaging microscopy (FLIM) analysis

FLIM measurements were conducted using an Olympus FVMPE-RS microscope, coupled with a two-photon Ti/sapphire laser operating at an 80 MHz repetition rate (MaiTaiHP, SpectraPhysics), along with a FLIM box system for lifetime acquisition (ISS, Urbana - Champaign). Paper samples were excited at 700 nm, and the emitted fluorescence was collected using a 30× planApo silicon immersion objective (NA = 1.0). A dichroic mirror below 570 nm was employed, complemented by a 510 nm filter with a ± 40 nm range. Calibration of the ISS FLIM box system was performed by measuring the known monoexponential lifetime decay of fluorescein at pH 11 (i.e., 4.0 nanoseconds). For calibration, a stock solution of 100 µmol/L fluorescein in ethanol was prepared and then diluted in 0.1 M NaOH for each measurement. During each FLIM measurement, a 512 × 512-pixel image was collected at a scanning speed of 10 µm/s. The laser power was not measured directly at the sample surface; instead, it was empirically adjusted based on the detected photon counts to ensure sufficient signal intensity while avoiding saturation and photodamage. The IR Ti: Sapphire laser was operated at 700 nm with a maximum output of 1.2 W. During acquisition, the laser power was set to 0.4% of its maximum output, corresponding to an estimated 4.8 mW before accounting for optical losses. The laser fluence at the sample surface was 0.113 J/cm^2 per pixel, which falls well within the safe range for two-photon microscopy. As additional precautions, each region was analysed for only a few seconds to minimise sample exposure. Depending on the fluorescence emission characteristics, between 20 and 30 frames were acquired per sample.

We used the phasor plot approach. For each pixel in the image, the fluorescence decay measured in the time domain is mapped onto a phasor plot, where each phasor is described by two coordinates: the real (G) and imaginary (S) components of the Fourier transform of the fluorescence decay[42,55]. These components are calculated at the angular repetition frequency (ω) of the laser. As a result, pixels with similar decay kinetics will cluster at similar coordinates in the phasor plot. Moreover, pixels containing a combination of two or more distinct decay components will lie along the linear trajectory between their individual phasors, reflecting a weighted linear combination of those contributions.

The real and imaginary components of the phasor are calculated as:

$$g_{i,j} = \frac{\int_0^T I(t)\cos(n\omega t)\,dt}{\int_0^T I(t)\,dt} \text{ and } s_{i,j} = \frac{\int_0^T I(t)\sin(n\omega t)\,dt}{\int_0^T I(t)\,dt} \tag{1}$$

where I(t) is the fluorescence intensity as a function of time, n is the harmonic, and ω is the angular frequency corresponding to the laser repetition rate. Alternatively, in the frequency domain, the phasor coordinates $g_{i,j}$ and $s_{i,j}$ can also be expressed in terms of the modulation $m_{i,j}$ and phase shift $\varphi_{i,j}$:

$$g_{i,j} = m_{i,j} \cdot \cos(\phi_{i,j}) \text{ and } m_{i,j} \cdot \sin(\phi_{i,j}) \tag{2}$$

In this representation, the phasors corresponding to monoexponential decays lie along the universal semicircle, centred at (0.5, 0) with a radius of 0.5. A phasor at (1, 0) corresponds to a lifetime of 0 ns, while a phasor at (0, 0) represents an infinite lifetime. Multiexponential decays fall inside this circle. Therefore, the fluorescence lifetime distribution of a given sample can be interpreted based solely on the position of its phasors within this universal semicircle[42,55]. Phasor plot analysis was carried out using SIM FCS 4 software (Laboratory for Fluorescence Dynamics, UC Irvine).

FTIR-ATR analysis

FTIR-ATR analysis was performed using a Cary 630 spectrometer to characterise the surface of the samples and detect compositional differences related to ageing. On the same sample, at least three measurements were taken in different areas; the spectra were analysed individually, and then they were subsequently averaged. The analyses were conducted at room temperature and humidity. Spectra were acquired in the range of 3700 to

$650\ cm^{-1}$ without the need for sample preparation. The spectral resolution was set at $4\ cm^{-1}$, and 256 scans were collected for background measurement and for the samples. The resulting spectra were then averaged to provide a representative measurement for each sample. The data were gathered using MicroLab Lite Software (v1.1), developed by Agilent Technologies.

The spectral region between 1800 and $1600\ cm^{-1}$ was selected as the diagnostic window for oxidation-related changes. All spectra were baseline-corrected and normalised to ensure comparability across samples. For each sample, the three individual spectra collected from different surface areas were analysed separately and then averaged to obtain a representative spectrum. Peak areas within the diagnostic region were calculated by numerical integration using Origin software (OriginLab Corporation, One Roundhouse Plaza, Suite 303, Northampton, MA 01060, USA), focusing on the absorption bands centred around 1745, 1680, and $1644\ cm^{-1}$. The integration limits were defined based on the full width of each band to capture the total absorbance signal. The resulting integrated area was used as a semi-quantitative indicator of chemical changes associated with ageing.

SEM-EDS analysis

SEM-EDS analysis was employed to obtain complementary information on the morphological and elemental features of the paper samples. While SEM-EDS is not sensitive to the molecular-level changes detected by FLIM or FTIR, it provides useful insights into the surface structure and elemental composition of the fibres. This allows for the detection of inorganic additives, surface contaminants, or morphological alterations induced by ageing, which could influence degradation mechanisms or affect optical measurements. Scanning Electron Microscopy (SEM) imaging analysis, including backscattered electrons (BSE) and Energy Dispersive Spectroscopy (EDS), was performed using a TM4000 Plus II microscope (Hitachi, Hitachi High-Tech Corporation, Tokyo, Japan). SEM-EDS data were acquired in medium vacuum at an accelerating voltage of 10 kV, with images recorded at magnifications of 600×. The instrument was equipped with a high-sensitivity 4-segment BSE detector, enabling the acquisition of X-ray maps of the main elements on the surface at a magnification of 100×. Given that we analysed both modern and historical samples, the samples were not subjected to any treatments, minimise destructiveness.

pH measurement

The pH measurement was conducted using a paper pH meter, Hanna Instruments HI99171, by placing the electrode in contact with the surface. At least three measurements were taken on the paper's surface.

Data availability

The datasets generated is not publicly available due to the ongoing patent application process, but are available from the corresponding author on reasonable request.

References

1. Di Turo, F. The chemistry behind paper restoration: diagnostic techniques and cutting-edge innovation. *ChemTexts* **11**, 7 (2025).
2. Małachowska, E., Dubowik, M., Boruszewski, P., Łojewska, J. & Przybysz, P. Influence of lignin content in cellulose pulp on paper durability. *Sci. Rep.* **10**, 19998 (2020).
3. Pinheiro, A. C., Sequeira, S. O. & Macedo, M. F. Fungi in archives, libraries, and museums: a review on paper conservation and human health. *Crit. Rev. Microbiol.* **45**, 686–700 (2019).
4. O'Sullivan, A. C. Cellulose: the structure slowly unravels. *Cellulose* **4**, 173–207 (1997).
5. Titubante, M. et al. Analysis and diagnosis of the state of conservation and restoration of paper-based artifacts: A non-invasive approach. *J. Cult. Herit.* **55**, 290–299 (2022).
6. Hajji, L. et al. Conservation of Moroccan manuscript papers aged 150, 200 and 800 years. Analysis by infrared spectroscopy (ATR-FTIR), X-ray diffraction (XRD), and scanning electron microscopy energy dispersive spectrometry (SEM–EDS). *Spectrochim Acta Mol. Biomol. Spectrosc.* **136**, 1038–1046 (2015).
7. Bicchieri, M., Biocca, P., Colaizzi, P. & Pinzari, F. Microscopic observations of paper and parchment: the archaeology of small objects. *Herit. Sci.* **7**, 47 (2019).
8. Manso, M. & Carvalho, M. L. Application of spectroscopic techniques for the study of paper documents: A survey. *Spectrochim Acta Part. B Spectrosc.* **64**, 482–490 (2009).
9. Małachowska, E., Pawcenis, D., Dańczak, J., Paczkowska, J. & Przybysz, K. Paper ageing: the effect of paper chemical composition on hydrolysis and oxidation. *Polymers* **13**, 1029 (2021).
10. Łojewski, T. et al. FTIR and uv/vis as methods for evaluation of oxidative degradation of model paper: DFT approach for carbonyl vibrations. *Carbohydr. Polym.* **82**, 370–375 (2010).
11. Vibert, C., Fayolle, B., Ricard, D. & Dupont, A. L. Decoupling hydrolysis and oxidation of cellulose in permanent paper aged under atmospheric conditions. *Carbohydr. Polym.* **310**, 120727 (2023).
12. Lovikka, V. A., Rautkari, L. & Maloney, T. C. Changes in the hygroscopic behavior of cellulose due to variations in relative humidity. *Cellulose* **25**, 87–104 (2018).
13. Emsley, A. M. & Stevens, G. C. Kinetics and mechanisms of the low-temperature degradation of cellulose. *Cellulose* **1**, 26–56 (1994).
14. Emsley, A. M., Heywood, R. J., Mushtaq, A., & Eley, C. M. On the kinetics of degradation of cellulose. Cellulose, 4(1), 1-5 (1997).
15. Jablonsky, M. & Šima, J. Oxidative degradation of paper – A minireview. *J. Cult. Herit.* **48**, 269–276 (2021).
16. Vornicu, N., Deselnicu, V., Bibire, C., Ivanov, D. & Doroftei, F. Analytical techniques used for the characterization and authentification of six ancient religious manuscripts (XVIII–XIX centuries). *Microsc Res. Tech.* **78**, 70–84 (2015).
17. Manso, M., Costa, M. & Carvalho, M. L. Comparison of elemental content on modern and ancient papers by EDXRF. *Appl. Phys. A.* **90**, 43–48 (2007).
18. Cheng, Q., Wang, S. & Harper, D. P. Effects of process and source on elastic modulus of single cellulose fibrils evaluated by atomic force microscopy. *Compos. Part. Appl. Sci. Manuf.* **40**, 583–588 (2009).

19. Piantanida, G., Bicchieri, M. & Coluzza, C. Atomic force microscopy characterization of the ageing of pure cellulose paper. *Polymer* **46**, 12313–12321 (2005).
20. Chakraborty, I. et al. An insight into microscopy and analytical techniques for morphological, structural, chemical, and thermal characterization of cellulose. *Microsc Res. Tech.* **85**, 1990–2015 (2022).
21. Foner, H. A. & Adan, N. The characterization of papers by X-Ray diffraction (XRD): measurement of cellulose crystallinity and determination of mineral composition. *J. Forensic Sci. Soc.* **23**, 313–321 (1983).
22. Capitani, D., Di Tullio, V. & Proietti, N. Nuclear magnetic resonance to characterize and monitor cultural heritage. *Prog Nucl. Magn. Reson. Spectrosc.* **64**, 29–69 (2012).
23. Bastone, S., F. Armetta, and E. Caponetti. "Physicochemical characterization of ancient paper and parchment with solid state nuclear magnetic resonance." Physicochemical Characterization Of Ancient Paper And Parchment With Solid State Nuclear Magnetic Resonance (2014).
24. Calahorra, M. E., Cortázar, M., Eguiazábal, J. I. & Guzmán, G. M. Thermogravimetric analysis of cellulose: effect of the molecular weight on thermal decomposition. *J. Appl. Polym. Sci.* **37**, 3305–3314 (1989).
25. Picker, K. M. & Hoag, S. W. Characterization of the thermal properties of microcrystalline cellulose by modulated temperature differential scanning calorimetry. *J. Pharm. Sci.* **91**, 342–349 (2002).
26. Nurazzi, N. M. et al. Thermogravimetric analysis properties of cellulosic natural fiber polymer composites: A review on influence of chemical treatments. *Polymers* **13**, 2710 (2021).
27. Nurazzi, N. M., et al. "Thermogravimetric analysis (TGA) and differential scanning calorimetry (DSC) of PLA/cellulose composites." Polylactic acid-based nanocellulose and cellulose composites. CRC Press. 145-164 (2022).
28. Ramiah, M. V. Thermogravimetric and differential thermal analysis of cellulose, hemicellulose, and lignin. *J. Appl. Polym. Sci.* **14**, 1323–1337 (1970).
29. Łojewska, J., Lubańska, A., Miśkowiec, P., Łojewski, T. & Proniewicz, L. M. FTIR in situ transmission studies on the kinetics of paper degradation via hydrolytic and oxidative reaction paths. *Appl. Phys. A*. **83**, 597–603 (2006).
30. Zotti, M., Ferroni, A. & Calvini, P. Microfungal biodeterioration of historic paper: preliminary FTIR and Microbiological analyses. *Int. Biodeterior. Biodegrad.* **62**, 186–194 (2008).
31. Olsson, A. M. & Salmén, L. The association of water to cellulose and hemicellulose in paper examined by FTIR spectroscopy. *Carbohydr. Res.* **339**, 813–818 (2004).
32. Ali, M., Emsley, A. M., Herman, H. & Heywood, R. J. Spectroscopic studies of the ageing of cellulosic paper. *Polymer* **42**, 2893–2900 (2001).
33. Evans, R. & Wallis, A. F. A. Cellulose molecular weights determined by viscometry. *J. Appl. Polym. Sci.* **37**, 2331–2340 (1989).
34. Mohtaschemi, M. et al. Rheological characterization of fibrillated cellulose suspensions via bucket Vane viscometer. *Cellulose* **21**, 1305–1312 (2014).
35. Gamelas, J. A. F. The surface properties of cellulose and lignocellulosic materials assessed by inverse gas chromatography: a review. *Cellulose* **20**, 2675–2693 (2013).
36. Dal Fovo, A. et al. Detecting early degradation of wood ultrastructure with nonlinear optical imaging and fluorescence lifetime analysis. *Polymers* **16**, 3590 (2024).
37. Dal Fovo, A. et al. Nonlinear imaging and vibrational spectroscopic analysis of cellulosic fibres treated with COEX® flame-retardant for tapestry preservation. *RSC Adv.* **12**, 26744–26752 (2022).
38. Chiriu, D. et al. Ageing of ancient paper: A kinetic model of cellulose degradation from Raman spectra. *J. Raman Spectrosc.* **49**, 1802–1811 (2018).
39. Možina, K., Černič, M. & Demšar, A. Non-destructive methods for chemical, optical, colorimetric and typographic characterisation of a reprint. *J. Cult. Herit.* **8**, 339–349 (2007).
40. Ferrara, V., Vetri, V., Pignataro, B., Martino, C., Sancataldo, G. & D. F. & Phasor-FLIM analysis of cellulose paper ageing mechanism with carbotrace 680 dye. *Int. J. Biol. Macromol.* **260**, 129452 (2024).
41. Kulpinski, P., Erdman, A., Namyslak, M. & Fidelus, J. D. Cellulose fibers modified by Eu3+-doped yttria-stabilized zirconia nanoparticles. *Cellulose* **19**, 1259–1269 (2012).
42. Digman, M. A., Caiolfa, V. R., Zamai, M. & Gratton, E. The phasor approach to fluorescence lifetime imaging analysis. *Biophys. J.* **94**, L14–L16 (2008).
43. Mecklenburg, Marion F., and Charles S. Tumosa. "Temperature and relative humidity effects on the mechanical and chemical stability of collections." ASHRAE journal 41: 77-83 (1999).
44. Havlínová, B., Katuščák, S., Petrovičová, M., Maková, A. & Brezová, V. A study of mechanical properties of papers exposed to various methods of accelerated ageing. Part I. The effect of heat and humidity on original wood-pulp papers. *J. Cult. Herit.* **10**, 222–231 (2009).
45. Zervos, S., Choulis, K. & Panagiaris, G. Experimental design for the investigation of the environmental factors effects on organic materials (Project INVENVORG). The case of paper. *Procedia - Soc Behav. Sci.* **147**, 39–46 (2014).
46. Marulier, C., Dumont, P. J. J., Orgéas, L., Du Roscoat, R., Caillerie & S. & D. 3D analysis of paper microstructures at the scale of fibres and bonds. *Cellulose* **22**, 1517–1539 (2015).
47. Dadmohamadi, K., Achachluei, M. M. & Jafari, M. T. The effect of cellulose nanofibers on paper documents containing starch and gelatine sizing. *Restaur Int. J. Preserv Libr. Arch. Mater.* **43**, 181–197 (2022).
48. Gamelas, J. A. F., Lourenço, A. F., Xavier, M. & Ferreira, P. J. Modification of precipitated calcium carbonate with cellulose esters and use as filler in papermaking. *Chem. Eng. Res. Des.* **92**, 2425–2430 (2014).
49. Han, J. S., Jung, S. Y., Kang, D. S. & Seo, Y. B. Development of flexible calcium carbonate for papermaking filler. *ACS Sustain. Chem. Eng.* **8**, 8994–9001 (2020).
50. Vibert, C. et al. Relationship between chemical and mechanical degradation of aged paper: fibre versus fibre–fibre bonds. *Cellulose* **31**, 1855–1873 (2024).
51. Barrett, Timothy, Mark Ormsby, and Joseph B. Lang. "Non-destructive analysis of 14th–19th century European handmade papers." Restaurator. International Journal for the Preservation of Library and Archival Material 37.2, 93-135 (2016).
52. Hunter, D. *Papermaking: the History and Technique of an Ancient Craft* (Courier Corporation, 1978).
53. Proietti, N. et al. Characterization of handmade papers (13th–15th century) from Camerino and Fabriano (Marche, Italy). *J. Cult. Herit.* **42**, 8–18 (2020).
54. ISO 5630-1. Paper and Board–Accelerated Ageing–Part 1: Dry Heat Treatment at 105 Degrees C." (1991).
55. Bernardi, M. et al. Phasor-FLIM-guided unraveling of ATRA supramolecular organization in liposomal nanoformulations. *Nanoscale* **15**, 19085–19090 (2023).

Acknowledgements

Author contributions

Conceptualization: F. C., P. P.; Methodology: F. D.T., A.M., F. C.; Formal analysis and investigation: F. D.T., A.

M.; Writing – original draft preparation: F. D.T.; Writing – review and editing: F. D. T., A. M., P. P., F. C.; Funding Acquisition: F. C.; Supervision: F. C. All authors read and approved the final version of the manuscript.

Declarations

Competing interests
The authors declare no competing interests.

Additional information
Supplementary Information The online version contains supplementary material available at https://doi.org/10.1038/s41598-025-16733-8.

Correspondence and requests for materials should be addressed to F.D.T. or F.C.

Reprints and permissions information is available at www.nature.com/reprints.

Publisher's note Springer Nature remains neutral with regard to jurisdictional claims in published maps and institutional affiliations.